International Conference on Mathematics, Computational Methods & Reactor Physics (M&C 2009)
Saratoga Springs, New York, May 3-7, 2009, on CD-ROM, American Nuclear Society, LaGrange Park, IL (2009)

OPTIMIZATION OF A COMPTON SUPPRESSION DETECTOR SYSTEM USING CdZnTe AND LIQUID SCINTILLATORS

M. M. Bourne, S. D. Clarke, and S. A. Pozzi
Department of Nuclear Engineering & Radiological Sciences
University of Michigan
Ann Arbor, MI 48109
clarkesd@umich.edu; mmbourne@umich.edu; pozzisa@umich.edu

A. Gueorguiev
ICX Radiation
Oak Ridge, TN 37830

ABSTRACT

The goal of this work is to explore and optimize a gamma-ray detection system combining cadmium-zinc-telluride (CZT) and organic liquid scintillator into a single detector for homeland security applications. The size and location of the CZT cell as well as the liquid scintillator are optimized to provide a high level of suppression (highest probability of secondary gamma-ray interaction in the scintillator) relative to detector portability. The optimization is performed with a newly-developed algorithm that relies on the output from a series of Monte Carlo simulations using MCNP-PoliMi. In the optimized detection system, the number of photopeak counts relative to partial-energy, Compton counts was increased by a factor of 3.0 relative to a bare CZT cell at a total detector weight of 16 lbs..

Key Words: Compton suppression, MCNP, MCNP-PoliMi

1. INTRODUCTION

The ability to detect clandestine nuclear activity has been the focus of much research in recent history. The detection of characteristic gamma rays is typically desirable for material identification because of the uniqueness of certain energy emissions. However, homeland security applications impose some challenging design goals for detection systems: inexpensive detectors that can operate in a myriad of conditions and collect meaningful data in a small measurement time. The current state-of-the-art gamma spectroscopy detector, high-purity germanium (HPGe), is expensive and requires constant cooling with liquid nitrogen (or cumbersome mechanical cooling pumps) to be effective. For these reasons, HPGe detectors are, in general, not ideal for homeland security applications. The goal of this work is to explore and optimize a gamma-ray detection system combining cadmium-zinc-telluride (CZT) and organic liquid scintillator into a single detector for homeland security applications. This system has been recently explored with a few different scintillation materials and showed FWHM energy resolutions less than 2% for ^{137}Cs gamma rays [1]. The benefit of this detector is its relatively low cost and room-temperature operation.

Compton suppression techniques have been explored in the past for several applications using various detectors [2, 3]. Here, small CZT cells are immersed in a volume of liquid scintillator.

The goal is to isolate only those events where the incoming gamma rays deposit their full energy in the CZT cell. Gamma rays that do not deposit their full energy in the CZT – those which undergo Compton scattering – will ideally interact in the surrounding liquid and produce a correlated scintillation pulse. These correlated counts can then be selectively ignored thereby isolating the photopeaks in the resulting gamma-ray spectrum. The size and location of the CZT as well as the liquid scintillator will be optimized to provide the best level of suppression (highest probability of secondary gamma-ray interaction in the scintillator) relative to detector portability.

2. MONTE CARLO MODELING

Monte Carlo codes have been widely used to design and analyze measurement systems of many types and configurations. However, when modeling the time-correlated events, the widely-used Monte Carlo code MCNPX has some limitations [4]. For this reason, the MCNP-PoliMi code was chosen for the simulations here.

2.1. Description of the MCNP-PoliMi Code

The MCNP-PoliMi code simulates time-analysis quantities, and includes a correlation between individual neutron interactions and the corresponding photon production [5]. Table I shows an excerpt from the detailed interaction data that is available from MCNP-PoliMi.

Table I. Excerpt from a MCNP-PoliMi collision output file.

History Number	Particle Number	Projectile Type	Interaction Type	Target Nucleus (atomic number)	Cell Number of Collision Event	Energy Deposited in collision (MeV)	Time (shakes)	Collision position (X)	(Y)	(Z)	Particle Weight	Generation Number	Number Scatterings
77	1	2 (gamma)	1 (Compton)	6	200 (liquid)	0.462227	0.02	4.78	-0.85	1.24	1	0	0
77	1	2	1	6	200	0.030576	0.03	2.35	0.57	1.47	1	0	1
77	1	2	1	6	200	0.010104	0.05	-3.44	-2.68	-0.84	1	0	3
182	1	2	1	52	100 (CZT)	0.45715	0.02	-0.21	0.41	0.26	1	0	0
182	1	2	1	1	200	0.064075	0.03	-1.71	2.85	3.94	1	0	1
757	1	2	3 (absorption)	48	100	0.661657	0.02	-0.69	-0.31	0.39	1	0	0

The event-by-event physics modeled in MCNP-PoliMi enables the simulation of detailed detection physics, which are typically disregarded in other simplified code systems. For example, from Table 1, history 757 shows a photoelectric absorption in the CZT detector, and history 182 shows a photon that scatters in the CZT then the liquid scintillator before escaping. The Compton suppression technique will reject history 182 while keeping the full-energy absorption of history 757. The physical behavior of each individual particle history will be analyzed in a similar fashion to compute the energy distributions of particle interactions in both the scintillation portion and the CZT portion of the detector volume.

2.2. MCNP-PoliMi Model Description

Figure 1 shows the CZT detector (in yellow) and the surrounding liquid scintillator (in blue) as they were modeled in MCNP-PoliMi. The ^{137}Cs point source is fixed 30 cm from the face of the liquid scintillator along the z-axis. The CZT cell, whose center is also aligned with the z-axis, has dimensions 1.3 × 1.5 × 0.5 cm and is radially-centered perpendicular to the *z*-axis. By varying the scintillator height and radius, along with the depth of the CZT cell (defined as the

distance from the face of the liquid scintillator to the front face of the CZT cell), the detector was optimized to have the smallest volume while still increasing the suppression ratio (the number of photopeak counts relative to Compton-continuum counts). The suppression ratio for each configuration was compared to the photopeak-to-Compton ratio for a bare cell. This ratio was used to optimize the detector; the target value for this ratio was chosen to be 3.0 by ICX Radiation.

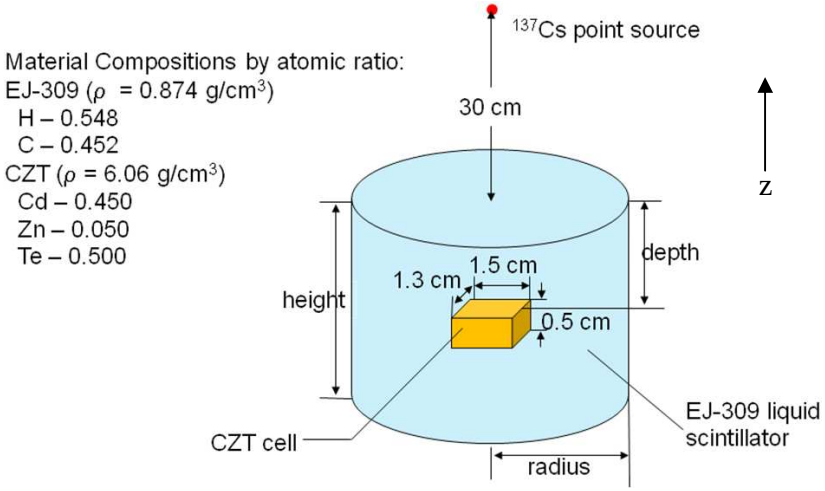

Figure 1. MCNP-PoliMi model of a CZT/liquid scintillator Compton suppression system.

3. DETECTOR DESIGN OPTIMIZATION

The detailed interaction data supplied by MCNP-PoliMI makes exact treatment of Compton suppression possible. A dedicated algorithm was written to perform the Compton suppression analysis on the MCNP-PoliMi collision output file. The algorithm, which was written in MATLAB, loads the entire output file and analyzes it history-by-history to determine which histories are counted and which are suppressed. There was not detection threshold in the liquid or CZT applied in these initla calculations. Figure 2 shows a typical spectrum generated by the post-processing algorithm. This spectrum gives the integral absorption histories and the integral scatter histories that were not suppressed by the liquid in each simulation. From this spectrum, the suppression ratio, Ψ, for trial *i* is given by

$$\Psi_i = \frac{IntAbs_i}{IntScatter_i}. \quad (1)$$

The suppression ratio is then used to calculate the figure of merit, Ω, used to optimize the detection system. This is given for trial *i* by

$$\Omega_i = \frac{\Psi_i}{\Psi_{BareCell}} \quad (2)$$

and was set to a target value of 3.0, corresponding to three times the suppression ratio relative to a bare cell.

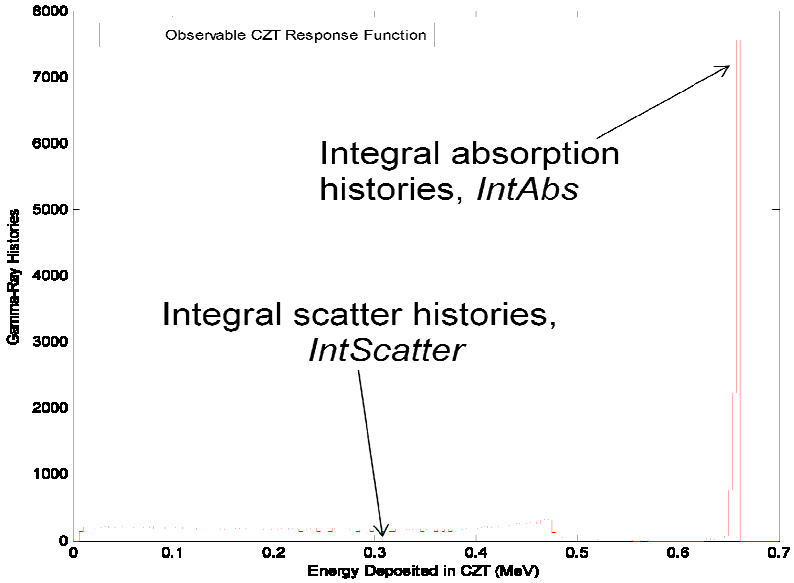

Figure 2. Sample CZT spectrum obtained from MCNP-PoliMi collision output file after Compton suppression technique is performed.

From this, the figure of merit per liquid volume, Γ, was maximized to incorporate detector portability into the optimization process:

$$\Gamma_i = \frac{\Omega_i}{LiqVol_i}. \tag{3}$$

First, $\Psi_{BareCell}$ was determined to be 0.33.

The CZT cell was initially centered lengthwise in the scintillator, and the scintillator dimensions were varied to the nearest centimeter to give the maximum value of Γ that still kept Ω at or above the target value of 3.0. As Table II shows, this occurred at Trial 1, with a scintillator radius of 12 cm, a scintillator height of 26 cm, and a cell depth of 12.5 cm. Next, the cell depth was varied by centimeter to assess the effect on Ω. It was discovered that Ω decreased as the depth was increased, and increased with a slight decrease in depth. The maximum Ω value was obtained at a depth of 8 cm. At this point, the target value of Ω was exceeded so the scintillator volume was decreased to further increase Γ while approaching the target value of Ω. This process was repeated until changing the depth did not increase Ω. This configuration, listed as Trial 5, was chosen as the optimum. It should be noted that there are many configurations in this range that result in an Ω value close to 3.0.

Table II: Select Trials Leading to Optimum Configuration

Trial Number	Radius (cm)	Height (cm)	Depth (cm)	Ψ	Ω	Γ
1	12	26	12.5	0.99	3.01	0.26
2	12	26	8	1.13	3.44	0.29
3	11	23	8	0.99	3.03	0.35
4	11	23	7	1.00	3.05	0.35
5	11	22	7	0.99	3.01	0.36

4. RESULTS

A theoretical spectrum for the CZT cell after suppression is generated by subtracting the number of histories that occur in *both* the CZT and the liquid from the total distribution. Afterwards, the total number of photopeak counts relative to the total counts in the Compton continuum is computed. Figure 3 shows a comparison of the optimum spectrum to the theoretical spectrum obtained from a bare CZT cell.

Because of the position of the CZT cell within the detector geometry, some incoming photons that would get absorbed by a bare CZT cell will be attenuated by the liquid and get suppressed. As a result, the detection system loses some overall photopeak efficiency as compared with a bare cell. For ^{137}Cs, the photopeak of the optimum configuration contained only 73% of the full-energy absorptions recorded by a bare CZT cell.

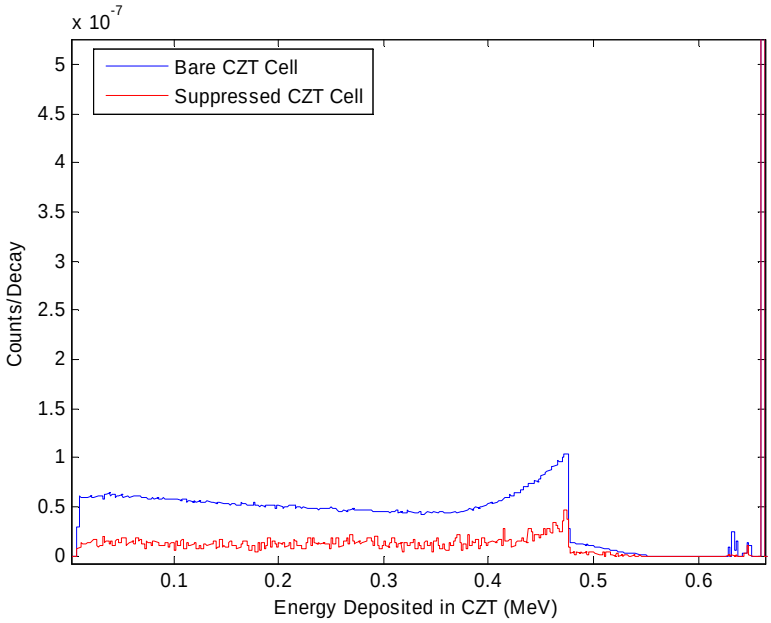

Figure 3. Comparison of an optimized Compton suppression system with a bare CZT cell response to a ^{137}Cs source.

To show the realistic detector response function exhibited by a CZT cell, work is being done to broaden the simulation photopeak to a near-Gaussian distribution. Previous work has shown that there are three components that sum to the distribution function of a CZT photopeak. The three components – a Gaussian (G), a Step (S), and a Tail (D) – are given by the following equations [6]:

$$G(E) = H_g e^{\left(\frac{-(E-E_0)^2}{2\sigma^2}\right)}, \tag{4}$$

$$S(E) = H_s H_g erf\left(\frac{E-E_0}{\sigma\sqrt{2}}\right), \tag{5}$$

and

$$D(E) = H_t H_g e^{\left(\frac{E-E_0}{T_s\sigma}\right)} erf\left(\frac{E-E_0}{\sigma\sqrt{2}} + \frac{1}{T_s\sqrt{2}}\right). \quad (6)$$

In these equations, a total of 5 parameters – E_0, σ, H_s, H_t, and T_s – are unknown, and H_g (common to all equations) is used as a scaling factor. This model was applied to measured data provided by ICX Radiation. By varying the parameter values and using H_g to match the photopeak obtained in the simulation results, the fit shown in Figure 4 was obtained. This fit matches the ICX data to an R^2 value of 0.9985.

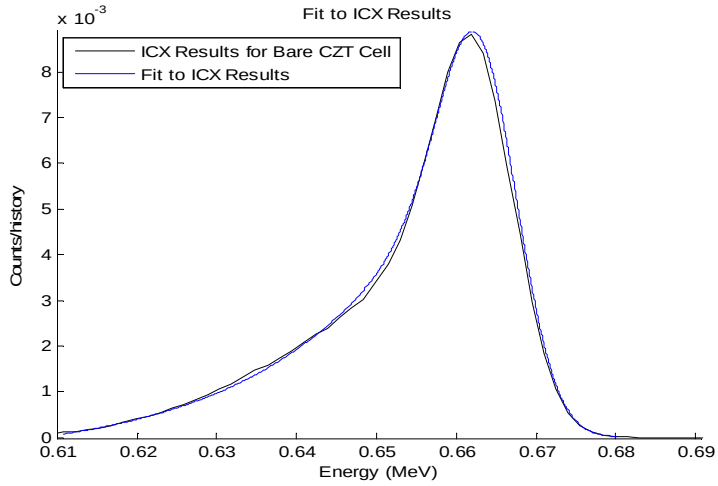

Figure 4. The obtained fit for the results supplied by ICX Radiation.

To verify the validity of this fit, the peak-to-Compton ratio – defined as the ratio of the broadened photopeak height to the mean value of the Compton continuum – was calculated for the fitted spectrum of the bare CZT detector response to ^{137}Cs seen in Figure 5a. This ratio has been experimentally determined to be approximately 6 for a bare CZT. A value of 5.99 was calculated from the MCNP-PoliMi simulation with the broadened photopeak. The peak-to-Compton ratio for the optimum suppressed cell seen in Figure 5b was calculated to be approximately 16. The quoted peak-to-Compton ratio for a typical HPGe detector at about 30 for ^{137}Cs.

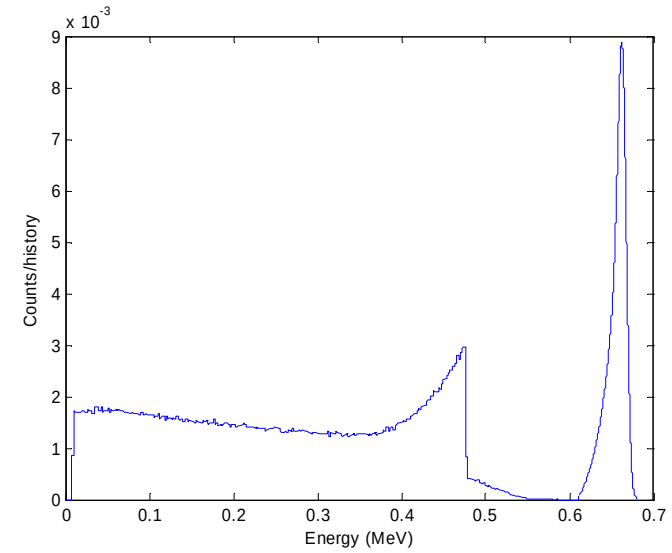

(a)

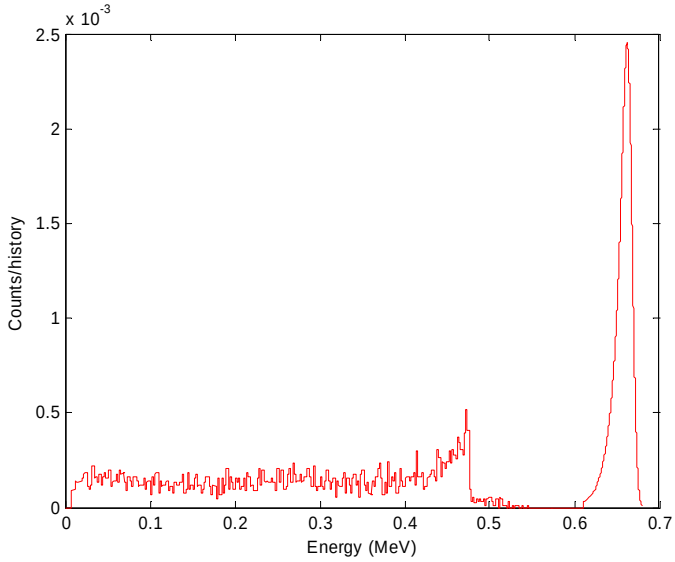

(b)

Figure 5: The full CZT spectra for the bare (a) and suppressed (b) cells after applying the obtained fit.

5. CONCLUSIONS

A Compton-suppression detector system using CZT and liquid scintillator has been optimized to provide the best level of suppression relative to detector portability. The MCNP-PoliMi code allows the tracking of each history throughout the proposed detector system. A specialized Matlab script was developed to calculate the level of Compton suppression for the Compton suppression system expressed as the ratio of photopeak counts to Compton-continuum counts. This suppression ratio was compared to the photopeak-to-Compton ratio for a bare CZT cell to determine an optimization parameter. This parameter was set to a target value of 3.0 and the

configuration was optimized with respect to the detector volume. The optimum configuration was determined to be with a scintillator radius of 11 cm, a scintillator height of 22 cm, and a CZT depth of 7 cm. However, there are many configurations in this range that result in a suppression ratio close to 3.0. The optimum dimensions correspond to a scintillator volume of 8 L and a total detector weight of approximately 16 lbs. Peak efficiency is also lost in the optimum configuration, recording only 73% of the full-energy absorptions recorded by a bare CZT cell.

The CZT photopeak has also been fitted with a near-Gaussian distribution from literature. The peak-to-Compton ratio of the fitted function was determined to be about 6, which matches the typical experimental results seen for a bare CZT cell. This makes it seem that the fitting technique gives a realistic detector response for the simulated detector. The same ratio for the optimum configuration was determined to be about 16.

The Compton suppression technique illustrated here provides more-clear isolation of the photopeak from a ^{137}Cs source above the Compton continuum. For other, more complex, radiation sources this technique could enhance the ability to currently resolve close-proximity peaks with a compact, room-temperature detector. In addition, the use of a liquid scintillator creates a detector system that is sensitive to neutrons as well as gamma rays; this feature has not yet been incorporated into the analysis.

REFERENCES

1. D.Y. Stewart, and Y.R. Ramachers, “CdZnTe Room-Temperature Semiconductor Operation in Liquid Scintillation Detector,” *J. Inst.*, doi: 10.1088/1748-0221/3/01/P01007, (2008).
2. Hyun-Je Cho, Yong-Sam Chung, and Young-Jin Kim, “Study on Prompt Gamma-ray Spectrometer Using Compton Suppression System,” *Nucl. Instr. and Meth. B*, **229**, pp. 499–507 (2005).
3. W. Scates, J.K. Hartwell, R. Aryaeinejad, and M.E. McIlwain, “Optimization Studies of a Compton Suppression Spectrometer Using Experimentally Validated Monte Carlo Simulations, “IEEE Nuclear Science Symposium Conference Record, pp. 550–554, (2005).
4. D. Pelowitz (ed.), 2005. “MCNPX User’s Manual, version 2.5.0,” Los Alamos National Laboratory, LA-CP-05-0369.
5. S. A. Pozzi, E. Padovani, and M. Marseguerra. ”MCNP-PoliMi: A Monte Carlo Code for Correlation Measurements,” *Nucl. Instr. and Meth. A*, **513**, pp. 550–558 (2003).
6. P. Mortreau and R. Berndt, “Characterization of Cadmium Zinc Telluride Detector Spectra – Application of the Analysis of Spent Fuel Spectra,” *Nuclear Instr. and Meth. A*, pp. 183-188 (2001).